

Metamorphosis of a nanowire: A 3-D coupled mode space NEGF study

S. M. Amoroso, V. P. Georgiev, E. Towie* and A. Asenov*

Device Modelling Group, University of Glasgow, G12 8LT, Glasgow, Scotland, UK

*Gold Standard Simulations Ltd, Glasgow G12 8LT, UK

e-mail: salvatore.amoroso@glasgow.ac.uk

ABSTRACT

In this paper we present a 3D coupled mode space NEGF study of the quantum features of a nanoscale Gate-All-Around (GAA) silicon transistor. The bottom oxide of the structure is parameterized in order to progressively transform the nanowire in a tri-gate FinFET and the electron transport studied for several Fin widths, back-biases voltages and electron effective masses.

SIMULATION METHODOLOGY

Simulations are carried out using the quantum transport module of the GSS TCAD simulator GARAND [1]. Accurate modelling of nanoscale GAA transistors can be tackled by coupled mode space (CMS) Non-Equilibrium Green's Function (NEGF) quantum transport approach [2,3], if a sufficient number of modes is included in simulation [4]. In our work we neglect all sources of incoherent scattering, such as phonon interaction, as they have a marginal impact on our results [5]. An effective-mass Hamiltonian is used in the discretized form of the NEGF equations so that the full crystal interactions are described by the parameters $m_{eff,i}$ which are derived from tight binding calculations of silicon band structure. Please note that the tight binding approach allows us to take into account the dependence of the electron band structure on the nanowire cross-section. The CMS method splits the quantum problem into the transversal and longitudinal spaces. The transversal space provides the cross-sectional wave functions and sub-band energies. The transport is solved in the product space of the longitudinal space with the mode space, allowing a considerable savings of computational resources with respect to a full 3D real-space approach [4]. Boundary conditions of the Green's function equations at the contacts, which are given throughout the contact self-energies, were defined by using the algorithm described in [6]. The electron density is used to calculate, self-consistently, the electrostatic potential through the Poisson's equation. The obtained solutions of the NEGF and Poisson equations are iterated in a Gummel-like loop until density and current converge.

RESULTS AND DISCUSSION

All calculations are performed at $V_G = 0.8V$ and $V_D = 50mV$. Fig.1 shows a schematic view of the nanowire progressively transforming into a FinFET. In Fig.2 we report the electron density and the potential along the length section for device A, for two values of applied back bias. When $V_B=0$, the electron density has a centroid close to the top interface, as the lateral gates are leveled at

the same height of the Si wire, preventing a good electrostatic control of the channel bottom. More uniform charge distribution in the channel is obtained by applying a positive back-bias. In this case the structure is nearly equivalent to a GAA nanowire. In Fig. 3 – Fig.4 we show results for the devices B-D featuring different bottom oxide thickness and/or channel height. In Fig.5 we offer an insight of the first five wave-functions (squared) with lowest eigenvalues for device D. The electron density of these tri-gate structures is more uniform along the channel height than the one observed in Fig.2a because the lateral gates in devices B-D penetrate deeper in the bottom oxide allowing the electric field streamlines to better embrace the channel. Moreover, increasing the ratio between channel height and channel width, the channel is majorly controlled by the lateral gates so that the inversion layer is dominant at the Fin sidewalls (see cross-section perpendicular to transport direction in each devices). However, Fig. 6 shows that this electron distribution can significantly be modified adopting different electron effective masses in our simulation. Increasing the ratio between m_z and m_y , the charge density redistribute from the Fin sidewalls to the Fin top, offering a results similar to the ones obtained from conventional TCAD simulations [7].

CONCLUSION

We have reported a thorough 3-D simulation study of quantum transport in multi-gate nanoscale devices showing how the electron wave features change in response to geometry, effective masses and applied back-biases variations.

REFERENCES

- [1] www.goldstandardsimulations.com
- [2] J. Wang et al., *A Three-Dimensional Quantum Simulation of Silicon Nanowire Transistors with the Effective Mass Approximation*, J. Appl. Phys. **96**, 2192, (2004)
- [3] G. Fiori et al., *Coupled Mode Space Approach for the Simulation of Realistic Carbon Nanotube Field-Effect Transistors*, IEEE TNT **6**, (2007).
- [4] A. Martinez et al., *A Comparison between a Fully-3D Real-Space Versus Coupled Mode-Space NEGF in the Study of Variability in Gate-All-Around Si Nanowire MOSFET*, Proc. of SISPAD 2009.
- [5] V. P. Georgiev, *Impact of Precisely Positioned Dopants on the Performance of an Ultimate Silicon Nanowire Transistor: A Full Three-Dimensional NEGF Simulation Study*, IEEE TED **60**, 965 (2013).
- [6] A. Martinez et al., *Variability in Si nanowire MOSFETs due to combined effect of interface roughness and random dopants: A full 3D NEGF study*, IEEE TED **57**, 1626, (2010).
- [7] L. Gerrer et al, *3-D Statistical Simulation Comparison of Oxide Reliability of Planar MOSFETs and FinFET*, IEEE TED **60**, 4008, (2013).

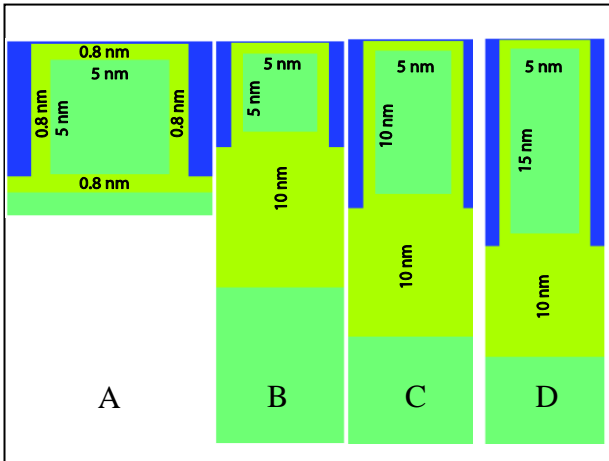


Fig. 1. Structure of the simulated devices. Thickness of the top, left and right SiO₂ and the channel width are constant. Bottom oxide and channel height change from device A to D.

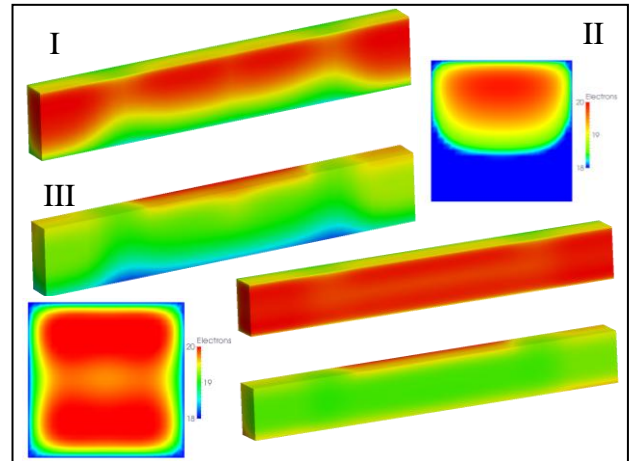


Fig. 2. Device A with bulk effective masses for Si: Electron density in a cut along the channel length (I) and on a cross-section perpendicular to the transport direction (II), and electrostatic potential (III). $V_B=0V$ (top), $V_B= 1.6V$ (bottom).

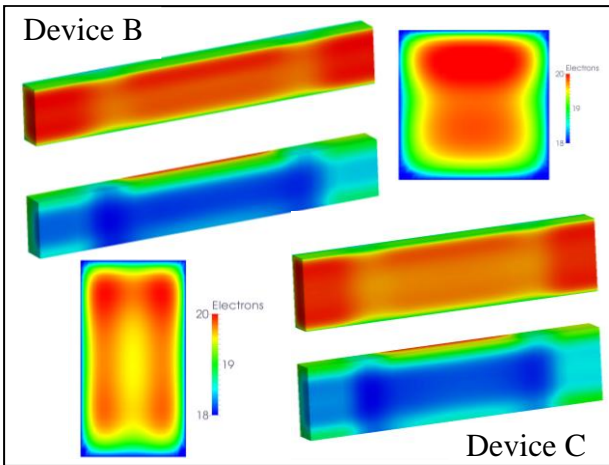


Fig. 3. The same as Fig.2, but for devices B and C.

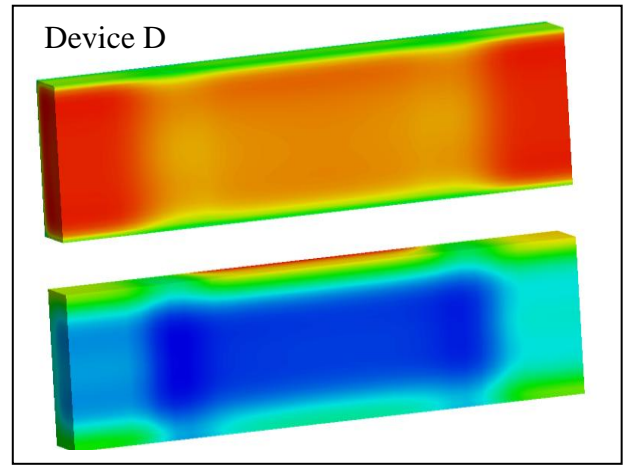


Fig. 4. Electron density (top) and potential (bottom) along the length of the channel for device D.

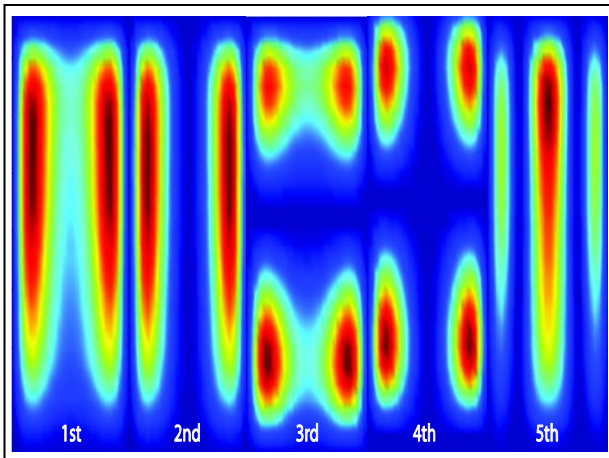


Fig. 5. Cross-section cut in the middle of the channel for device D showing the five wavefunctions with the lowest energy. The effective masses correspond to usual bulk effective masses – $m_z^*=0.916m_0$ and $m_y^*=0.191m_0$.

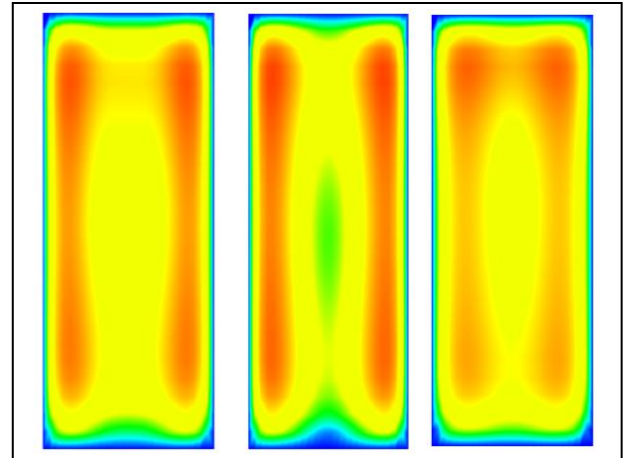


Fig.6. Electron density in the cut along the cross-section for device D: a) with bulk effective masses – $m_z^*=0.916m_0$ and $m_y^*=0.191m_0$; b) $m_z^*=1.03m_0$ and $m_y^*=0.30m_0$; c) $m_z^*=2.03m_0$ and $m_y^*=0.10m_0$.